



QSAR, HQSAR AND DOCKING BASED DESIGNING OF PYRIDO [1, 2] A BENZIMIDAZOLE DERIVATIVES AS ANTI-MALARIAL AGENTS

Vikram Choudhary¹, Shourya Pratap^{*1, 2}, Shweta Mittal³, Sunil Kumar⁴

¹School of Pharmacy, Devi Ahilya Vishwavidyalaya, Takshila Campus, Khandwa Road (Ring Road) Indore, Madhya Pradesh, India

²Department of Pharmaceutical Chemistry, B. Pharmacy College, Rampura Kakanpur, Godhra, Gujrat, India

³Delhi Institute Of Pharmaceutical Sciences and Research -Mehrauli-Badarpur Rd, Sector 3, Pushp Vihar, New Delhi, India

⁴Department of Pharmacy, Central University of Rajasthan, Rajasthan, India

*Corresponding author: shouryayadav122@gmail.com

ABSTRACT

The docking and Quantitative structure-activity relationship (QSAR) studies of Pyrido [1, 2] a benzimidazoles nucleus were performed on a series of 40 analogues. The training set consisting of 32 molecules in Comparative Molecular Field (CoMFA), Comparative molecular similarity indices analysis (CoMSIA) and Hologram QSAR(HQSAR) models gives cross-validated r^2 (q^2) and (S.E) standard error of 0.613, 0.980 and 0.021 and conventional on MMFF 94 q^2 0.785 r^2 0.942 and (S.E) standard error 0.033 respectively. The predicted r^2 values 0.882, 0.788 and 0.867 for Comparative Molecular Field Analysis (CoMFA) modeling, CoMSIA modeling and HQSAR modeling respectively, shows these generated models are appropriate for further designing. In addition to this work the docking studies were performed on Protein model of *Plasmodium falciparum* (PDB 2ANL) which further explore the binding affinity towards active site of protein receptor. The results guide us for the creation of more potent and effective compounds towards strain of *Plasmodium falciparum* relative to chloroquine.

Keywords: Benzimidazole, CoMFA, CoMSIA, HQSAR, PDB 2ANL, *Plasmodium falciparum*, QSAR.

1. INTRODUCTION

Genus *Plasmodium* (P) is a bloodborne protozoan that caused Malaria and is communicated by the Anopheles mosquito, among the more than 70 species among the five genera *Plasmodium* currently known to infect humans are *P. falciparum*, *P. Vivax*, *P. Malaria*, *P. Knowles*, and *P. Ovale* [1-6]. The most significant of these in terms of mortality is *P. falciparum*, although *P. Vivax* also has an enormous influence on population concerning morbidity, According to the World Health Organization report 2017, there were an estimated 445000 deaths from malaria globally [7]. To overcome the failures of monotherapy and to address the different underlying defects of the pathology of malaria, modern drugs are effectively being used, either singly or in combination as adjuncts to dietary therapeutic measures. Because of their pharmacological activities, heterocyclic compounds have gained much importance in recent years. The presence of the benzimidazole ring ensures the promising anti-malarial activity [8, 9]. By implicating *in-silico* designing approaches to a series of the nucleus, there is an enormous possibility to develop some novel

promising entities. Quantitative structure-activity relationship (QSAR) is used as a commanding tool for assessment of the contribution of different fragments and properties of molecules with biological activity. Several attempts are made previously to create the relation between benzimidazole structure and its reducing potential. In 3DQSAR (CoMFA and CoMSIA) different descriptors (electrostatic, hydrophobic, steric, donor and acceptor) were used for statistical model generation. HQSAR fragment distinction map also shows good statistical relation between structure and biological activity docking studies reveals the ligand interaction to the active protein site. This helps us to evaluate enzyme-ligand interactions at the molecular level with different amino acid bindings necessary for a physiological response. Our current efforts are to spotlight the 3D QSAR (CoMFA and CoMSIA), 2D QSAR (HQSAR), and docking studies of molecule for designing.

2. MATERIAL AND METHODS

The software ChemDraw Ultra ver.7.0 SYBYL X 2.0

SYBYL X 2.1 was used for docking studies. A selected compound series of 40 Pyrido [1, 2] benzimidazoles were developed by Makala A. et.al [9]. The IC_{50} and compounds of this series are shown in table 1. The effective concentration values (IC_{50}) was converted to

negative log from (pIC_{50}) and used for QSAR model generation. CoMFA (fig. 1), CoMSIA (fig.2), and HQSAR (fig. 3) models were generated using 8 compounds for the test set and 32 compounds for the training set.

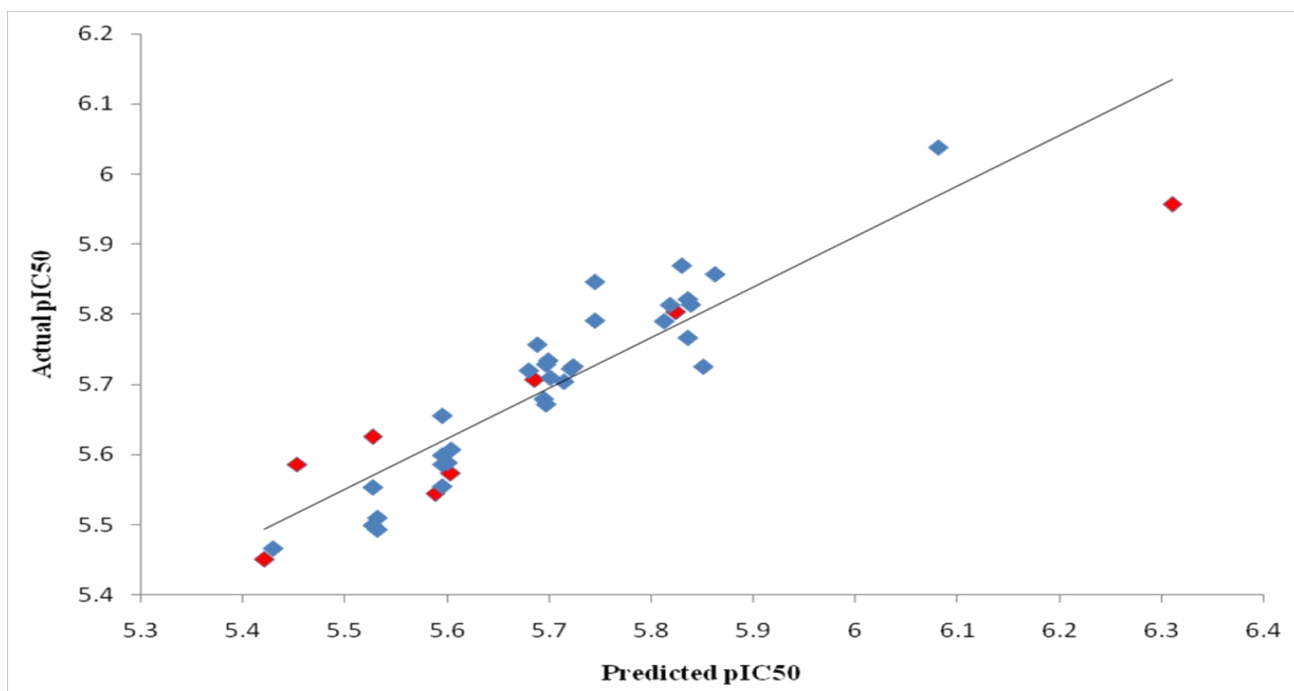


Fig. 1: CoMFA graph between actual and predicted pIC_{50}

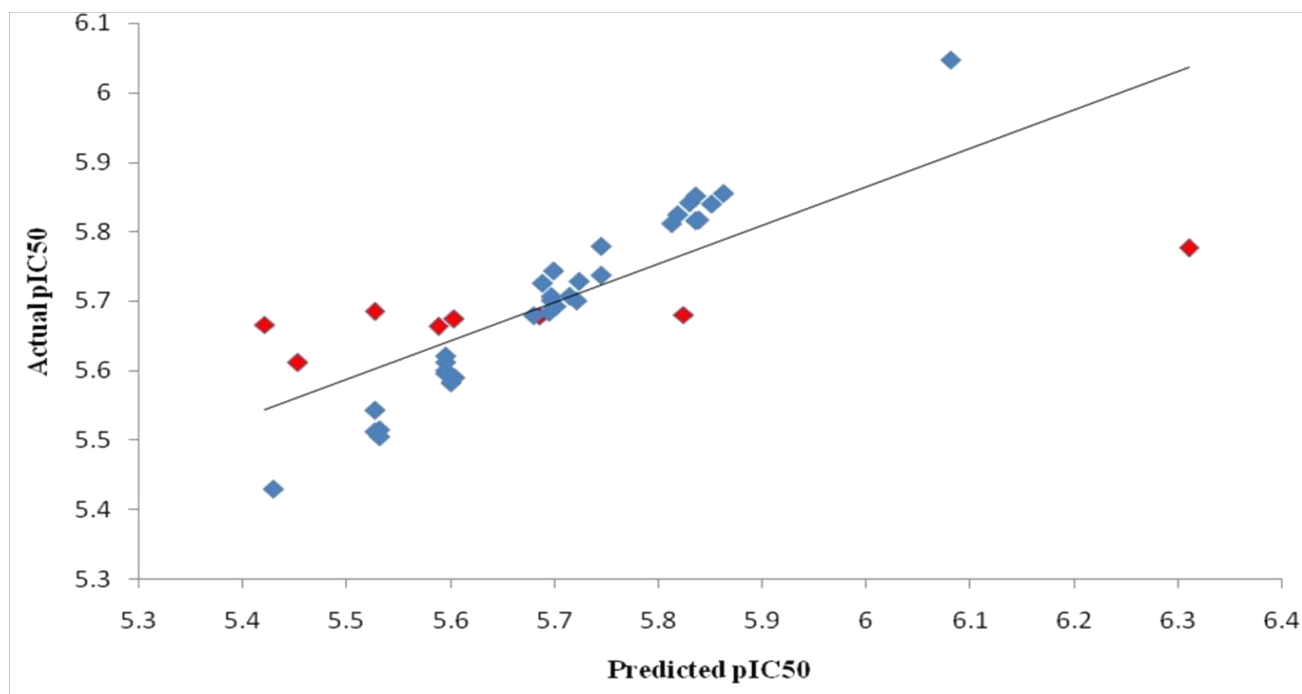


Fig. 2: CoMSIA graph between actual and predicted pIC_{50}

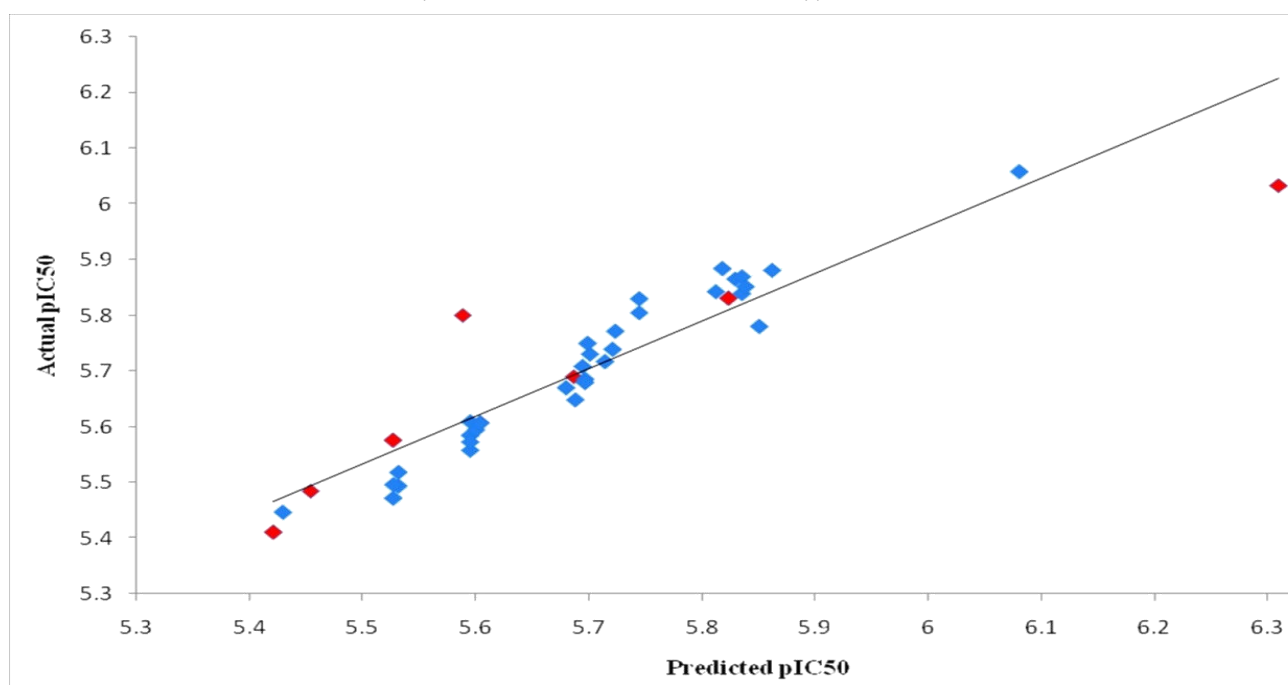


Fig. 3: HQSAR graph between actual and predicted pIC_{50} Test Set  Training Set 

Table 1: Anti malarial activity (IC_{50}) with CoMFA, CoMSIA, and HQSAR predicted activities and residual values

Compound No.	HQSAR A/B/DA			CoMFA		CoMSIA	
	Actual pIC_{50}	Predicted pIC_{50}	Residual value	Predicted pIC_{50}	Residual Value	Predicted pIC_{50}	Residual Value
1	5.7447	5.8299	-0.0852	5.8462	-0.1015	5.7376	0.0071
2	5.7447	5.8047	-0.06	5.7911	-0.0464	5.7793	-0.034
3	6.0809	6.058	0.0229	6.0375	0.0434	6.0477	0.0332
4	5.8623	5.881	-0.0187	5.8571	0.0052	5.8555	0.0068
5	5.5952	5.5848	0.0104	5.6557	-0.0605	5.6211	-0.025
6	5.5952	5.6092	-0.014	5.5864	0.0088	5.596	-0.008
7	5.8297	5.8653	-0.035	5.8694	-0.0397	5.8421	-0.0125
8	5.6968	5.6855	0.0113	5.7288	-0.032	5.707	-0.0102
9	5.8508	5.7803	0.0705	5.7255	0.1253	5.8403	0.0105
10*	5.8239	5.831	-0.0071	5.8031	0.0208	5.6803	0.1436
11	5.6882	5.6486	0.0396	5.7569	-0.0687	5.7262	-0.038
12	5.5317	5.4941	0.0376	5.4936	0.0381	5.5148	0.0169
13	5.5317	5.5185	0.0132	5.5103	0.0214	5.5049	0.0268
14	5.7235	5.7718	-0.0483	5.7259	-0.0024	5.7287	-0.052
15	5.6003	5.5948	0.0055	5.5887	0.0116	5.5826	0.0177
16	5.7212	5.7392	-0.018	5.7225	-0.0013	5.7007	0.0205
17	5.7011	5.7306	-0.0295	5.7096	-0.0085	5.6926	0.0085
18	5.5952	5.5579	0.0373	5.5993	-0.0041	5.6122	-0.017
19	5.8356	5.8395	-0.0039	5.7667	0.0689	5.8518	-0.016
20	5.8356	5.8693	-0.0337	5.8214	0.0142	5.8163	0.0193
21*	6.3098	6.033	0.2768	5.9569	0.3529	5.7767	0.5331
22	5.6038	5.6064	-0.0026	5.6073	-0.0035	5.59	0.0138
23*	5.6038	5.607	-0.0032	5.5729	0.0309	5.674	-0.0702
24	5.8182	5.8841	-0.0659	5.8133	0.0049	5.8248	-0.006

25*	5.6861	5.69	-0.0039	5.7071	-0.021	5.6788	0.0073
26	5.8386	5.8515	-0.0129	5.814	0.0246	5.8172	0.0214
27	5.8125	5.8428	-0.0303	5.7902	0.0223	5.812	0.0005
28	5.6799	5.6702	0.0097	5.72	-0.0401	5.6794	0.0005
29	5.5272	5.4722	0.055	5.4996	0.0276	5.5121	0.0151
30	5.5272	5.4966	0.0306	5.5538	-0.0266	5.5431	-0.015
31	5.699	5.7499	-0.0509	5.7342	-0.0352	5.7438	-0.044
32	5.5952	5.5729	0.0223	5.5551	0.0401	5.6001	-0.004
33	5.7144	5.7172	-0.0028	5.7042	0.0102	5.7075	0.0069
34	5.6946	5.7086	-0.014	5.6796	0.015	5.6843	0.0103
35*	5.5272	5.576	-0.0488	5.6259	-0.0987	5.6851	-0.1579
36*	5.4535	5.485	-0.0315	5.5866	-0.1331	5.6115	-0.158
37	5.6968	5.6797	0.0171	5.6718	0.025	5.7013	-0.004
38*	5.5884	5.8	-0.2116	5.5441	0.0443	5.6629	-0.0745
39	5.4295	5.4469	-0.0174	5.4667	-0.0372	5.4294	0.0001
40*	5.4214	5.41	0.0114	5.4504	-0.029	5.6658	-0.2444

*Test compounds

2.1. Structural alignment

Now the sequence of the compound is energy minimized engage technique which used for energy minimization to represent with a name *i.e.*, distance-dependent dielectric and conjugate gradient technique which measure Tripos force field and Gasteiger Huckel charge with convergence basis having energy was 0.01kcal/mol. CoMFA, CoMSIA, and HQSAR models were initiated on SYBYL X 2.1 [10, 11].

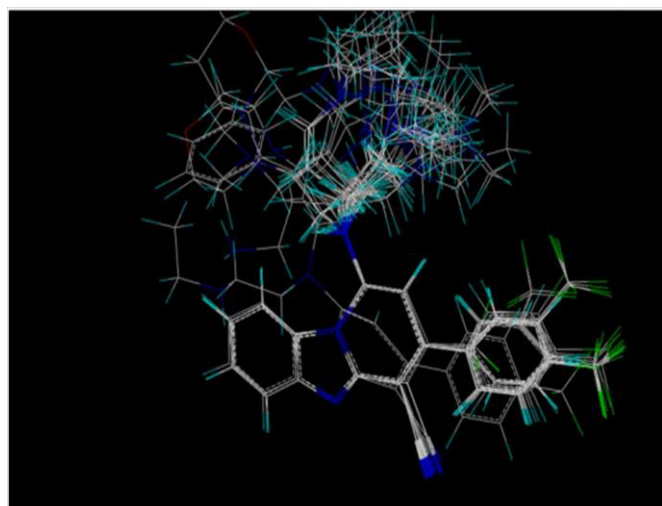


Fig. 4: Structural alignment of compounds

2.2. CoMFA

The aligned training set of molecules was positioned inside grid boxes with a grid spacing value of 2Å (default distance) in all Cartesian direction and CoMFA steric and electrostatic fields were calculated. The interaction energies for each molecule were calculated at each grid

point using. The (vdW interaction) and electrostatic (coulombic values) fields were calculated at each intersection on the regularly spaced grid. The cutoff value for both steric and electrostatic interaction was set to 30Kcal/mol. Different charges Gasteiger, Gasteiger-Huckel, Delre, Pullman, MMFF94, and Formal charges were used to generate the CoMFA models. The best CoMFA model was generated on MMFF 94 charge. PLS analysis was performed with cross-validation (LOO) and then using no validation with a column filtering of 2.0 the superiority of the CoMFA models can be estimated by the obtained q^2 and the predictive capability of the models can be determined by r^2_{pred} . The projected accomplishments for the test set were obtained from the model produced by the training set [12, 13].

2.3. CoMSIA

CoMSIA QSAR method overcomes the deficiencies of Lennard-Jones and Coulomb potentials which are used in the CoMFA method because it uses Gaussian function to calculate the interaction energy between compounds and probe atom. Steric, electrostatic, hydrophobic, H-bond donor, and H-bond acceptor fields are used in CoMFA analysis for charge calculation. The CoMSIA models were generated using an sp^3 hybridized carbon atom having +1 charge, attenuation factor 0.3, and Vander Walls radius of 1.4 Å. This probe atom is placed in every point of the lattice to calculate the different CoMSIA field which is steric, electrostatic, and hydrophobic, H-bond donors and H-bond acceptor fields. The different CoMSIA models gave the highest

statistical value in SEHD (steric, electrostatic, hydrophobic, and donor field) combination at MMFF94 charge, CoMSIA employs Gaussian type distance dependence and similarity indices for the generation of clear and smooth contour maps [14, 15]. The final CoMSIA model was generated with the highest cross-validated r^2 (q^2) and convention r^2 with an optimum number of components.

2.4. HQSAR

The new technique 2D-QSAR which employs predictive variables of the biological activity of specialized fragment fingerprints. The 3D alignment does not require HQSAR and 3D alignment is sensitive to three parameters concerning hologram generation, including hologram length, fragment size, and fragment distinction. The fragments distinct are atoms (A), bonds (B), connections (C), hydrogen atoms (H), chirality (Ch), and donor (D). Initially, the default fragment size of 4 to 7 used to develop various models and different components, then based on the different fragment distinctions determined by the first step, the models were developed using different fragment sizes. The models with better results were applied to different fragment sizes and component number [16, 17]. From the above fragment size 2 to 5, in A/B/Ch/D distinct and several components, six observed the better statistical results were obtained.

2.5. Docking analysis

Surflex Dock module in SYBYL X2.0 software was used for Molecular docking studies. The retrieval of the structure of PDB name along with their inhibitor has been done by RCSB Protein Data Bank (PDB entry code: 2ANL). The protein structure was subjected to energy minimization and charge calculation (AMBER7FF99). After that, the known complex Protein structure was used to investigate and validate

the docking protocol. All unusual ligands and water molecules were removed. The bloat values and threshold values were set as 1 and 0.5 respectively for the generation of protocol and that position was considered as the active sites for potential receptor's binding [18].

3. RESULTS AND DISCUSSION

3.1. CoMFA and CoMSIA statistical results

Different parameters such as correlation coefficient (r^2), cross-validated correlation coefficient (q^2), and standard error of estimate were taken into consideration while building the QSAR model. Leave one out (LOO) cross-validation was performed to find out cross-validated r^2 (q^2) and several components. After the cross-validation runs non-cross-validation run was performed to find out other parameters. Best generated CoMFA and CoMSIA models in Pullman charges having q^2 values of 0.783 and 0.892 respectively. The r^2 value of CoMFA and CoMSIA analysis were 0.834 and 0.879 respectively. CoMFA steric field contribution was 0.899 while electrostatic field contribution was 0.401, which indicates the dominant role of electron donation and electron-withdrawing group inactivity. CoMSIA analysis gives better statistical results in terms of cross-validated r^2 (q^2). The CoMSIA analysis explores more fields as compare to CoMFA analysis. CoMSIA analysis reveals steric, and electrostatic contributions so steric, hydrophobic, and donor contributions which were listed in table 2. The contributions of steric, electrostatic, donor, acceptor, and hydrophobic fields of the best CoMSIA model were 0.141, 0.390, 0.207, 0.444, and 0.119 respectively. The correlation graph between experimental pIC_{50} and predicted pIC_{50} for different CoMFA, CoMSIA, and HQSAR model was shown in fig. 6 and fig. 7. The predicted and residual values of the models were shown in table 2.

Table 2: The PLS statistics of CoMFA and CoMSIA models for Anti-malarial activity indicating the best model and field contribution

Statistical parameters	CoMFA	CoMSIA	Field contribution	CoMFA	CoMSIA
q^2 (Cross validated)	0.783	0.892	Steric	0.899	0.141
r^2	0.834	0.879	Electrostatic	0.401	0.390
F value	51.903	91.279	Donor	-	0.207
SEE	0.021	0.040	Acceptor	-	0.444
Number of component	6	7	Hydrophobic	-	0.119
Pred R^2	0.882	0.788			

3.2. CoMFA and CoMSIA contour map analysis

The PLS CoMFA contours maps in terms of generation of common steric and electrostatic potential by taking compound 12 having the greatest anti-malarial activity of the dataset suggesting that CoMFA steric interaction is favored by steric/bulky groups in phenyl ring and CF₃ group attached to it at the 4th position at R₁ 5th position near CN group in phenyl ring and the 1st position phenyl ring at R₂ (Green), while steric burden at ring near R₃ position (Yellow) are supposed not to be favorable. CoMFA electrostatic interaction is favored by electrostatic substitution at phenyl ring at 4th position of CN group, 5th & 6th position of phenyl ring B and near the R₃ substitution ring (Blue), While electrostatic substitution at 4th position of CF₃ and above the benzimidazole ring at R₃ position (Red) are expected to be unfavorable (fig. 5 and fig. 6).

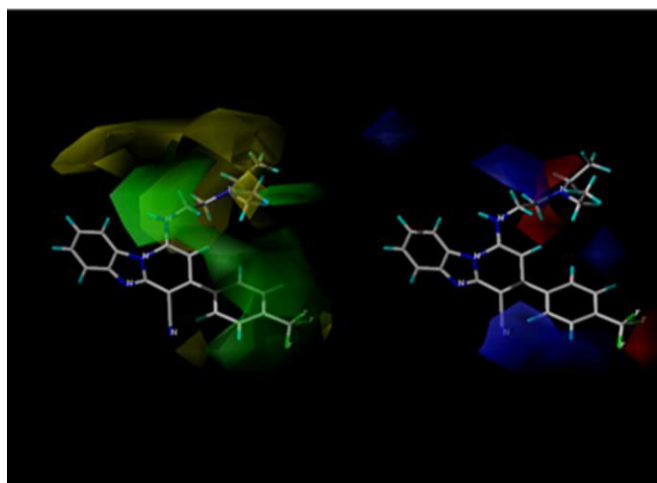


Fig. 5: CoMFA contour Maps of compound 12

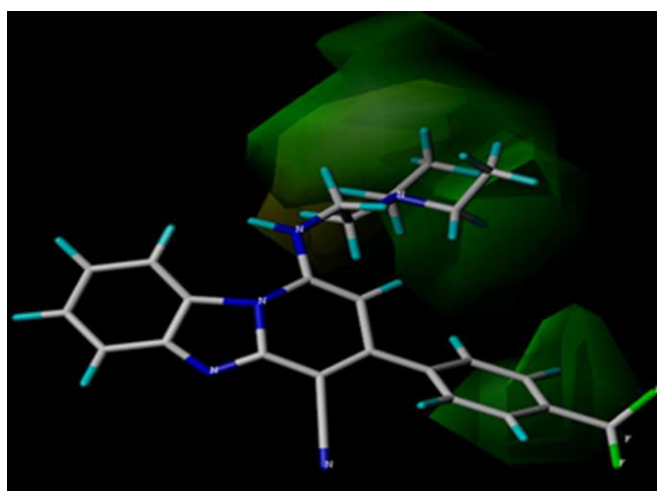


Fig. 6(a): CoMSIA contour map (steric)

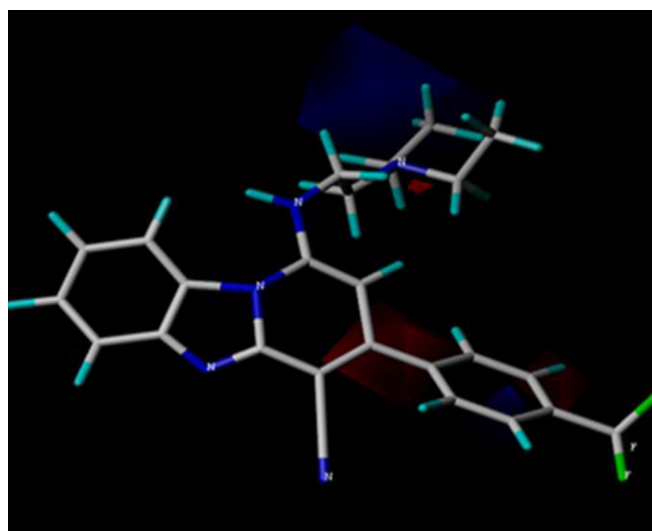


Fig. 6(b): CoMSIA contour map (Electrostatic)

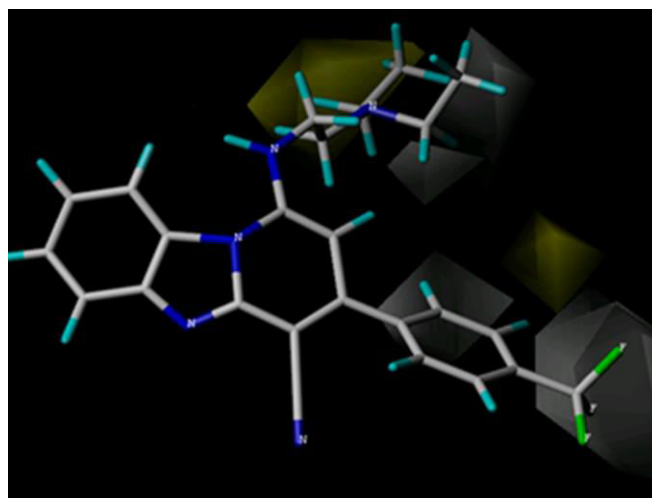


Fig. 6(c): CoMSIA contour map (Hydrophobic)

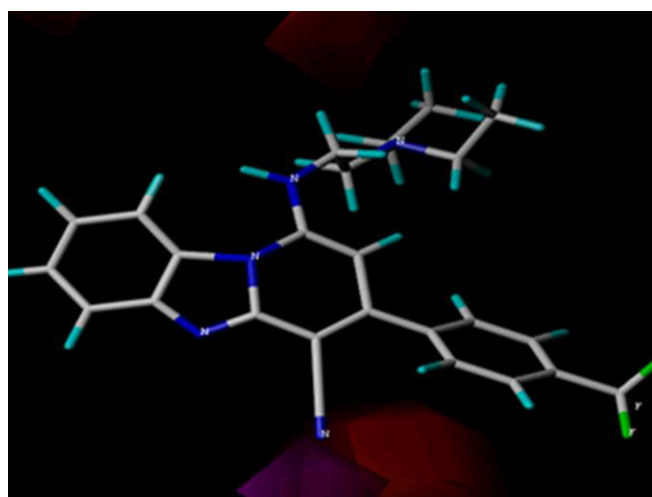


Fig. 6(d): CoMSIA contour map (Donor)

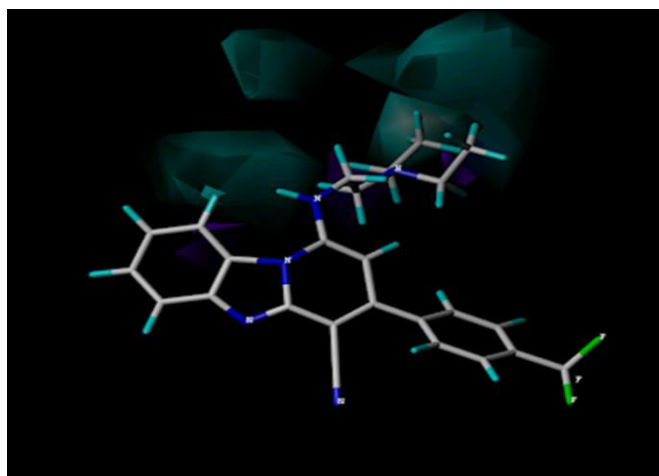


Fig. 6 (e): CoMSIA contour map (Acceptor)

Pose analysis of compound 12 with CoMFA steric parameter suggested that phenyl ring and CF_3 group attached to it at the 4th position at R_1 , 5th position near CN group in phenyl ring, and at the 1st position phenyl ring at R_2 is not favoring the bulky group addition, while R_3 is supported by the addition of bulky groups.

The PLS contours from CoMSIA analysis were carried out, taking the most active compound number 12. Steric interaction showed that phenyl ring at 1st position of R_2 is supposed to be not favoring (Yellow) while near phenyl ring at R_1 at 3, 4 and 5 position and above the benzimidazole ring at the R_3 position of the ethyl ring (Green) steric group. The addition of a small nonbulky group at phenyl ring at 1st position of R_2 is supposed to enhance antimalarial activity while at a near phenyl ring at R_1 at 3, 4 and 5 position and above the benzimidazole

ring at the R_3 position, enhance the antimalarial activity, electrophilic interaction showed that above the benzimidazole ring at the R_3 position strongly favored by electron donor (Blue) and while the phenyl ring at R_1 shows withdrawal group (Red). Hydrophobic phenyl ring at 1st position, the 3rd position of CF_3 , and the benzimidazole ring at the R_3 position do not support the hydrophobic substitution (White). Hydrophobic substitution is also supposed to support activity at position 8th benzimidazole and interaction showed that above the benzimidazole ring at the R_3 position (Magenta) and acceptor group at 4th of the CN position of a ring.

3.3. HQSAR studies

For optimum anti-malarial activity choose the best HQSAR model was generated using Atom(A) bonds(B) Donor (D) Acceptor (A) as fragment distinction parameters and 2-5 as the fragment size, showing $q^2 = 0.935$ and $r^2 = 0.971$ at 6 optimum numbers of components and 199 hologram lengths were selected for anti-malarial. The another best HQSAR model was developed using atoms (A) bonds (B) Chirality Hydrogen (Ch) Donor-Acceptor (DA) as fragment distinction parameters and 2-5 as the fragment size, showing $q^2 = 0.935$ and $r^2 = 0.971$ at 6 optimum numbers of components and 151 hologram lengths were selected (table 3). It is interesting to note that the both best model of data set was generated when along fragments (*i.e.*, 6-10 for anti-malarial activity) were not considered. Notably, there is an inverse relationship between the side chain length and the potency.

Table 3: Summary of statistical parameters of HQSAR study

S. No.	Statistical parameters	Fragment distinctions	
		Model 1(A/B/DA)	Model 2(A/B/Ch/DA)
1.	Fragment size	2-5	2-5
2.	r^2 best cv	0.971	0.971
3.	q^2 best full	0.935	0.935
4.	r^2 Ensemble	0.967	0.967
5.	Standard error	0.025	0.025
6.	Number of components	6	6
7.	Best hologram length(bin)	199	151

3.4. HQSAR contour maps analysis:

In the HQSAR contour map (fig. 7), red and orange color shows a negative contribution while green and yellow color shows a positive contribution to activity. In the HQSAR contour of compound number 12 orange

and red contour is seen in the phenyl ring which shows the phenyl ring 4, 5 positions near the CN group enhance the antimalarial activity and yellow color near R_3 position above the imidazole ring positive contribution to activity.

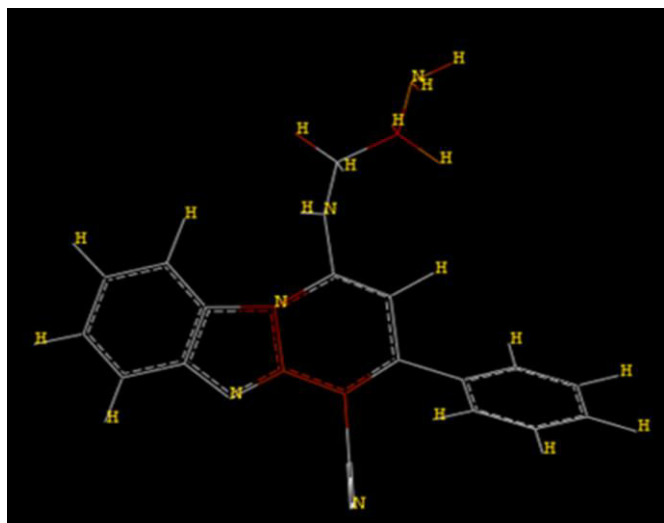


Fig. 7: HQSAR Molecular fragment pose compound 12

3.5. Pharmacophore Mapping

Genetic algorithm with linear assignment of hyper-molecular alignment of datasets (GALAHAD) was employed to initiate the pharmacophore models. All the structure in the training set were prepared by the following procedures; the structures were checked for

bond orders, hydrogen atoms were added and minimization procedures was implemented using the MMFF94, force-field GALAHAD was run for sixty generation with a population size of one hundred. The rest of the framework was placed as default values. The generated models were evaluated by a test database; several parameters were employed for model evaluation.

3.6. Docking studies

Surflex Dock module in SYBYL X2.0 software was used for Molecular docking studies. The retrieval of the structure of PDB name along with their inhibitor has been done by RCSB Protein Data Bank (PDB entry code: 2 ANL). The protein structure was subjected to energy minimization and charge calculation (AMBER7FF99). After that, the known complex Protein structure was used to investigate and validate the docking protocol. All unusual ligands and water molecules were removed. The bloat values and threshold values were set as 1 and 0.5 respectively for the generation of protocol and that position was considered as the active sites for potential receptor's binding (table 4 & figs.8-13).

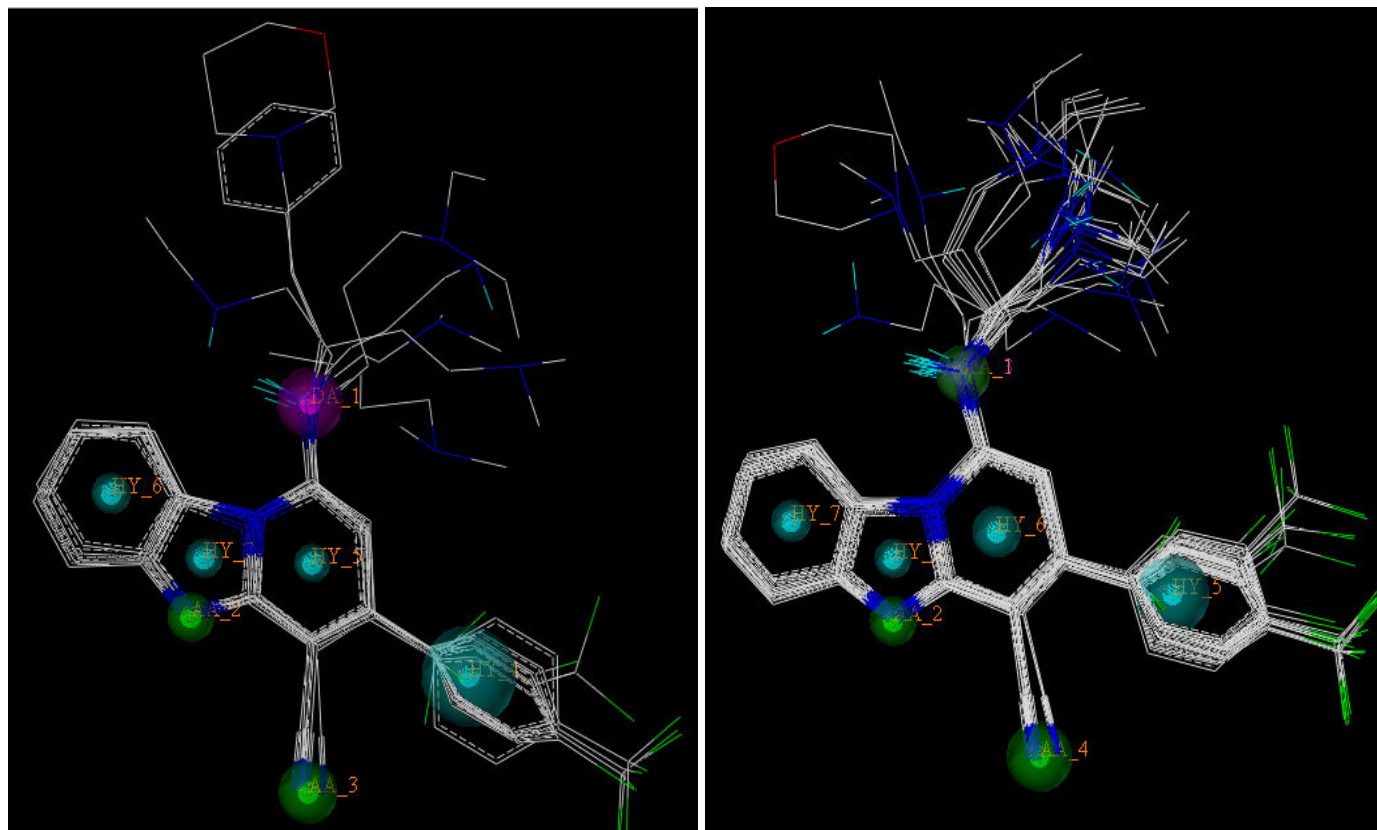


Fig. 8: Pharmacophore model alignment of all test and training compound

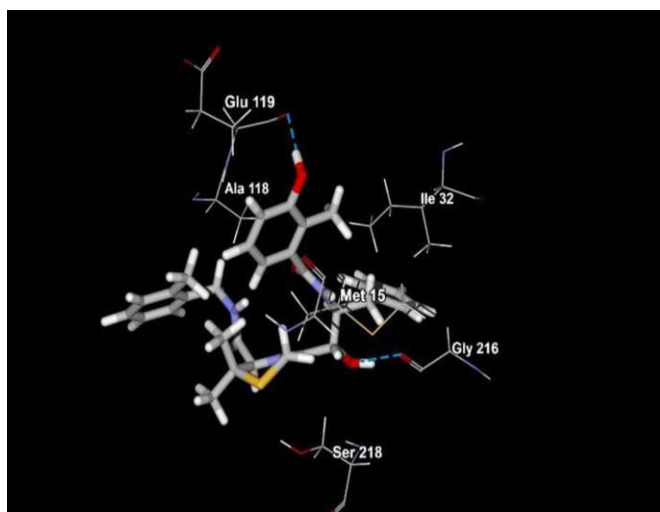


Fig. 9: Docking pose of most active compound

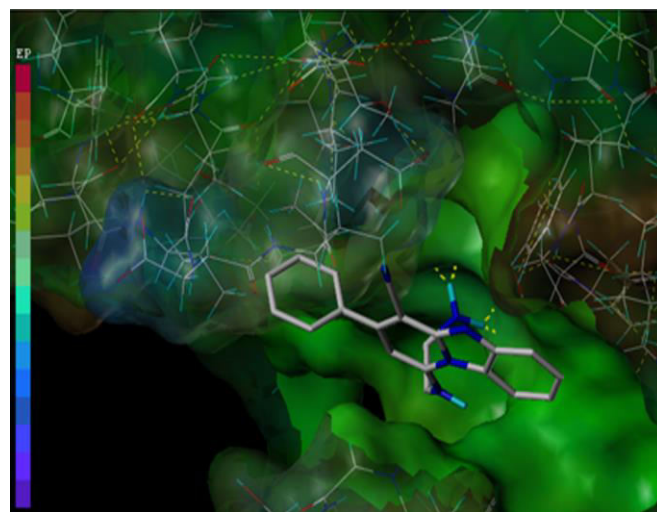


Fig. 12: Docking Lipophilic interaction

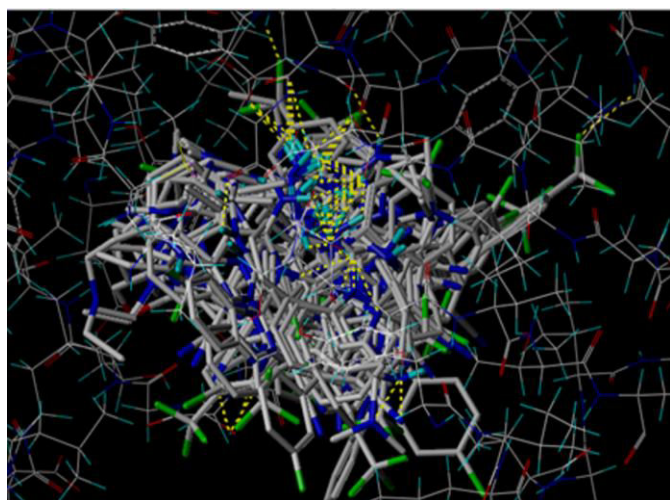


Fig. 10: Docking of all compounds

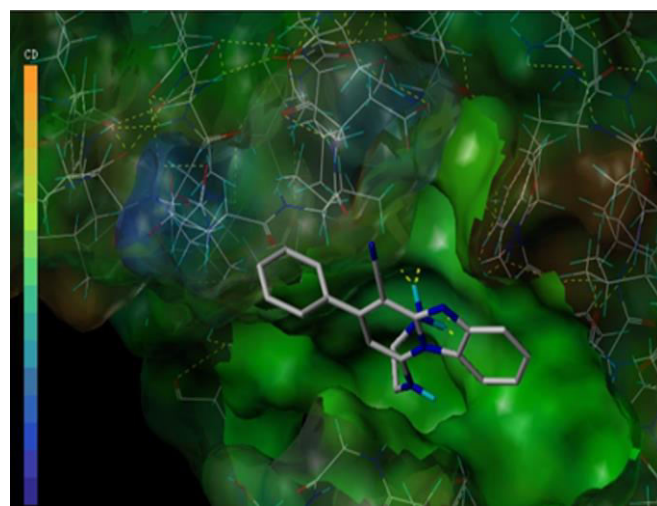


Fig. 13: Docking Electrophilic interaction

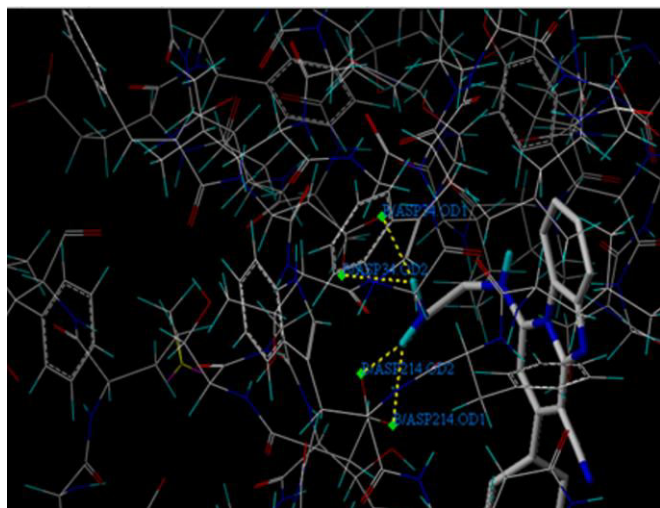


Fig. 11: Docking of compound 3

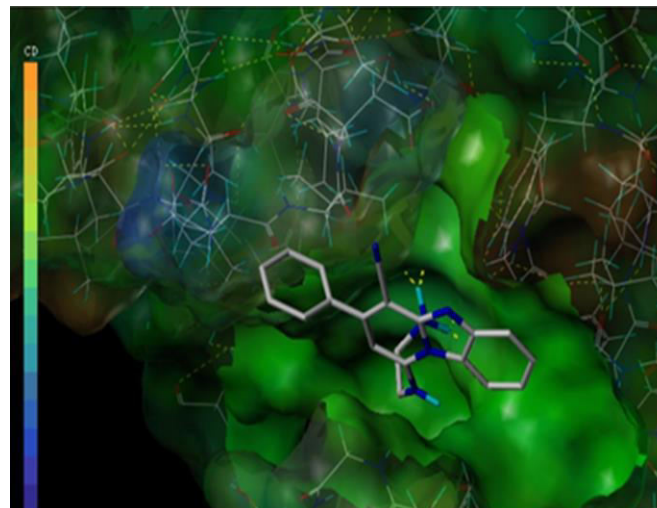


Fig. 14: Docking Cavity depth interaction

Table 4: Docking results training set and test set

S. N	COM-POUNDS	TOTAL SCORE	CRASH	POLAR	D-SCORE	PMF-SCORE	G-SCORE	CHEM-SCORE	C-SCORE	GLOBAL-CSORE
1	Comp 1	5.43	-1.22	3.49	-123.3	-47.73	-140.0	-22.23	1	2
2	Comp 2	5.49	-1.38	3.52	-133.3	-58.73	-151.8	-27.23	4	4
3	Comp 3	5.64	-1.50	3.54	-128.5	-59.02	-151.1	-26.83	3	3
4	Comp 4	4.57	-0.40	3.47	-101.2	-54.12	-75.46	-19.66	1	1
5	Comp 5	5.73	-1.43	0.92	-146.0	-22.31	-194.0	-21.74	5	5
6	Comp 6	5.05	-1.27	0.37	-109.8	-8.22	-180.0	-19.37	2	2
7	Comp 7	5.09	-1.29	1.39	-128.9	-41.65	-169.3	-24.18	4	4
8	Comp 8	4.78	-0.66	1.43	-120.5	-37.32	-156.5	-18.09	2	2
9	Comp 9	4.60	-1.32	0.93	-131.6	-50.55	-158.1	-24.92	2	2
10	Comp 10*	4.70	-1.30	1.00	-127.9	-51.38	-162.5	-24.40	4	2
11	Comp 11	4.62	-1.57	0.00	-150.0	-27.85	-178.3	-20.19	3	3
12	Comp 12	6.71	-1.81	0.76	-181.5	-18.16	-242.2	-27.79	4	4
13	Comp 13	6.33	-1.06	0.00	-146.7	-44.32	-199.3	-22.60	5	5
14	Comp 14	5.25	-1.37	0.00	-128.5	-27.61	-204.3	-22.24	4	4
15	Comp 15	5.33	-0.81	1.49	-138.3	-46.62	-176.5	-20.15	4	4
16	Comp 16	6.45	-1.71	0.00	-159.8	-36.90	-225.8	-22.65	5	5
17	Comp 17	5.61	-3.20	2.05	-160.2	-17.35	-236.5	-22.05	4	4
18	Comp 18	5.66	-1.65	0.02	-133.1	5.342	-230.1	-21.97	4	4
19	Comp 19	6.16	-1.21	1.61	-141.4	-48.70	-189.5	-24.06	5	5
20	Comp 20	5.79	-1.69	3.68	-133.3	-35.96	-150.3	-21.76	4	4
21	Comp 21*	5.62	-1.08	2.29	-141.8	-40.05	-168.5	-25.95	5	3
22	Comp 22	6.44	-1.50	1.63	-153.0	-46.85	-225.6	-21.39	5	5
23	Comp 23*	5.24	-0.66	2.39	137.4	-26.79	-158.5	-23.71	3	3
24	Comp 24	5.12	-1.11	1.44	-141.0	-27.08	-174.7	-21.90	5	5
25	Comp 25*	5.94	-1.76	1.32	-153.6	-26.74	-224.7	-22.43	4	5
26	Comp 26	5.74	-0.87	1.22	-130.5	-41.83	-181.8	-21.38	4	4
27	Comp 27	5.38	-2.04	1.06	-137.9	-38.80	-164.9	-25.78	5	5
28	Comp 28	4.70	-1.34	0.04	-133.9	-31.41	-165.8	-17.40	4	4
29	Comp 29	6.67	-2.14	1.12	-184.4	-32.20	-249.4	-30.69	5	5
30	Comp 30	5.86	-1.50	1.51	-158.4	-50.42	-238.4	-23.92	5	5
31	Comp 31	5.81	-1.42	0.00	-143.2	1.613	-219.1	-18.44	3	3
32	Comp 32	4.91	-1.04	0.02	-133.1	-15.41	-202.7	-16.52	3	3
33	Comp 33	5.68	-1.73	0.00	-162.0	-46.42	-251.2	-25.91	5	5
34	Comp 34	5.60	-1.81	0.00	-128.9	-33.93	-207.3	-21.47	4	4
35	Comp 35*	6.41	-1.50	1.56	-168.6	-46.59	-230.8	-29.91	4	5
36	Comp 36*	7.32	-2.08	1.70	-171.5	-11.50	-223.9	-29.50	4	4
37	Comp 37	5.40	-0.62	1.51	-141.6	-51.55	-172.8	-20.59	5	5
38	Comp 38*	5.62	-1.50	2.47	-155.9	-51.63	-200.2	-23.43	4	5
39	Comp 39*	5.46	-2.52	0.00	-181.4	-8.280	-247.5	-24.95	3	4
40	Comp 40	5.09	-0.81	0.00	-144.4	-33.29	-197.1	-20.23	4	4

*Test compounds

4. CONCLUSIONS

This study describes QSAR and docking studies for the designing of novel antimalarial agents. The QSAR methods, CoMFA, CoMSIA, and HQSAR were used to find out the relationship between the structures of all compounds and activities to get new clues to develop new potent antimalarial agents. The CoMFA, CoMSIA, and HQSAR models showed meaningful statistically significant results in terms of internal validation (q^2) of Pyrido [1,2] benzimidazole derivatives. We successfully got three rational and predictive QSAR models due to the high q^2 obtained from these different QSAR methods. The explored CoMFA and CoMSIA models

help us to give information about the favorable and unfavorable region while HQSAR gives information about the positive, the negative and intermediate contribution of substructural fingerprint requirements for imparting the biological activity. The CoMFA, CoMSIA, and HQSAR contour maps revealed sufficient information to understand the structure-activity relationship (SAR) and to recognize.

5. ACKNOWLEDGEMENT

We would like to convey our heartiest thanks to Dr. E. Manivannan, Associate Professor, School of Pharmacy for providing facilities.

Funding

Funding was provided by University Grants Commission, New Delhi & All India Council for Technical Education, New Delhi.

6. REFERENCES

1. Center for Disease Control. <http://www.cdc.gov/malaria/history/index.html> [Accessed on 10th December, 2020].
2. Krogstad DJ, Guerrant RL, Walker DH, Weller PF, et al. *Churchill Livingstone*, 1999; **1**:736-766.
3. Service M, Townson H, Gilles H, Warrell DA, et al. *Essential Malariology*, 2002; **4**:59-84.
4. Gurarie D, Zimmerman PA, King CH, et al. *J. Theor. Biol*, 2006; **240**:185-199.
5. Mayxay M, Pukrittayakamee S, Newton PN, White NJ, et al. *Trends Parasitol*, 2004; **20**:233-240.
6. Zimmerman PA, Mehlotra RK, Kasehagen LJ, Kazura JW, et al. *Trends Parasitol*, 2004; **20**:440-447.
7. WHO 2017, World Malaria report.10-17(<http://www.who.int/malaria/publications/worldmalaria-report-2017/en/>).
8. Ndakala AJ, Gessner RK, Gitari PW, October N, White KL, Hudson A, et al. *J. Med. Chem*, 2011; **54(13)**:4581-4589.
9. Torres-Gomez H, Hernandez-Nunez L, Leon Rivera I, Guerrero-Alvarez J, Cedillo-Rivera R, Moo-Puc R, et al. *Bioorg. Med. Chem. Lett*, 2008; **18**:3147-3151.
10. Sybyl-X. Molecular Modeling Software Packages, Version 2.0, TRIPOS Associates, Inc: St. Louis, 47 MO, USA, 2012.
11. Xu F, Yang Z, Ke Z, Xi L.M, Yan QD, Yang WQ, et al. *Bioorg. Med. Chem. Lett*, 2016; **26**:4580-4586.
12. Geladi P, Kowalski BR, et al. *Anal. Chim. Acta*, 1986; **185**:1-17.
13. Neves BJ, Bueno RV, Braga RC, Andrade CH. *Bioorg. Med. Chem*, 2013; **23**:2436-2441.
14. Jaes C, Sook K, Won-Hee L, et al. *Bio Pharm*, 2008; **31**:154-158.
15. Xu CX, Cui SY, Liu MC, Hu ZD, Fan BT, et al. *Eur. J. Med. Chem*, 2004; **39**:745-753.
16. Vyas VK, Ghate M, Gupta N, et al. *Arab. J. Chem.*, 2017; **10**:2182-2195.
17. Li J, Li S, Bai C, Liu H, Gramatica P, et al. *J. Mol. Graphics & Modeling*, 2013; **44**:266-277.
18. Keri RS, Hiremathad A, Budagumpi S, Nagaraja BM, et al. *Chem. Bio & D. Design*, 2015; **86**:19-65.
19. RCSB Protein Data Bank. <http://www.rcsb.org> [accessed on 10th December,2020].
20. Clemente JC, Govindasamy L, Madabushi A, Fisher SZ, Moose RE, Yowell CA, et al. *Acta Crystallogr, Sect. D: BiolCrystallogr*, 2006; **62**:246-256.
21. CS Chem Office, 2002. Cambridge Soft Corporation. Version 7.0, Software Publishers Association, 1730 Mstreet, NW, Suite 700, Washington, DC.20036, 452.